

Anomalous softening of phonon-dispersion in cuprate superconductors

Saheli Sarkar,¹ Maxence Grandadam,¹ and Catherine Pépin¹

¹*Institut de Physique Théorique, Université Paris-Saclay, CEA, CNRS, F-91191 Gif-sur-Yvette, France.*

A softening of phonon-dispersion has been observed experimentally in under-doped cuprate superconductors at the charge-density wave (CDW) ordering wave vector. Interestingly, the softening occurs below the superconducting (SC) transition temperature T_c , in contrast to the metallic systems, where the softening occurs usually below the CDW onset temperature T_{CDW} . An understanding of the ‘anomalous’ nature of the phonon-softening and its connection to the pseudo-gap phase in under-doped cuprates remain open questions. Within a perturbative approach, we show that a complex interplay among the ubiquitous CDW, SC orders and life-time of quasi-particles associated to thermal fluctuations, can explain the anomalous phonon-softening below T_c . Furthermore, our formalism captures different characteristics of the low temperature phonon-softening depending on material specificity.

The ‘pseudo-gap’ phase [1–8] of the under-doped high-temperature copper-oxide based superconductors (cuprates) remains incomprehensible even after decades of research, by and large due to a complex interplay of several symmetry broken orders [9, 10]. A universally present translational symmetry broken order in the cuprates is a charge-density wave (CDW) order [11–23]. Since its discovery, the CDW order has become fundamentally important due to growing evidences of its close relation to the pseudo-gap phase, although a full knowledge about the CDW order and its relation to the pseudo-gap phase remains incomplete. One leading approach to unravel the relation, is to study the phonon-spectrum which couples to electronic degrees of freedom, thus leaving fingerprints associated to the electronic-structure.

The phonon-spectrum has been largely studied in metallic systems, where the the charge-correlations soften the phonon-spectrum giving rise to the ‘Kohn-anomaly’ [24]. In one dimensional metals [25–27] and in some transitional metal dichalcogenides [28], this softening grows towards zero [Fig. 1] and a full phonon-softening occurs at the CDW wave-vector (Q) below CDW ordering temperature T_{CDW} , reflecting the origin of CDW order in them. With a similar outlook, the phonon-spectrum has been measured even in cuprates using different experimental techniques, like inelastic x-ray scattering and inelastic neutron scattering [17, 29–38]. All of these experiments have observed a partial phonon-softening [Fig. 1] associated to Q in several cuprates, only below the superconducting transition temperature T_c , in stark contrast to the metallic systems [27, 28, 39, 40]. The occurrence of phonon-softening below T_c is hence referred to as ‘anomalous’ phonon-softening.

The anomalous phonon-softening indicates a close connection between the CDW and superconductivity in under-doped cuprates. Such a connection between CDW and superconductivity have been widely discussed in various theoretical studies [41–44]. Supporting evidences of this connection can also be found in several experiments [11, 13, 45, 46]. Notably, a recent proposal [47], based on the fractionalization of a pair-density wave (PDW) or-

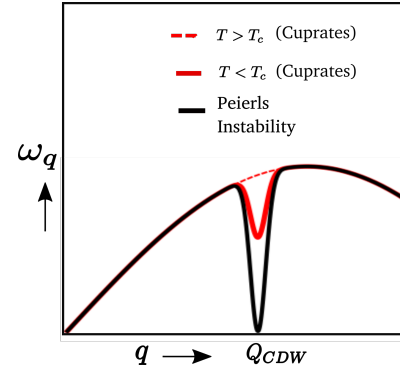


FIG. 1. Schematic representation of a full softening in metals and a partial softening in under-doped cuprates below T_c .

der [48, 49], advocates that for temperatures above T_c , a growing amount of fluctuations in CDW and superconductivity arising from a connection between them, can provide potential explanation to the pseudo-gap phase.

While earlier studies [43, 50–52] discussed the role of CDW, superconductivity and associated fluctuations on the electronic-spectrum, their effect on the bosonic excitations, especially phonons, remain an outstanding question and perhaps can give a more complete understanding of the CDW orders in cuprates. In this letter, we incorporate simultaneous effects of CDW, superconductivity and thermal fluctuations on the phonon-spectrum. In our model, we mimic the fluctuations by introducing an inverse life-time of quasi-particles [52, 53] and take its temperature dependence phenomenologically [53] based on earlier studies, which can capture various crucial aspects of the electronic spectrum in the pseudo-gap phase. We find that a strong phonon-softening occurs only below T_c , thus explaining the anomalous nature of the phonon-softening seen in experiments. Additionally, we also show that at low temperatures, different temperature dependence of the superconducting (SC) gap and inverse life-time of quasi-particle give contrasting effects on the strength of the phonon-softening.

We start with a total Hamiltonian H_{tot} [54], given by

$H_{tot} = H_e + H_{ph} + H_{e-ph}$, with,

$$\begin{aligned}
H_e &= \sum_{k,\sigma} \xi_k c_{k,\sigma}^\dagger c_{k,\sigma} + \sum_{k,\sigma} (\chi_k c_{k+Q,\sigma}^\dagger c_{k,\sigma} + h.c.) \quad (1) \\
&+ \sum_k (\Delta_k c_{k,\uparrow}^\dagger c_{-k,\downarrow}^\dagger + h.c.), \\
H_{ph} &= \sum_q \omega_q (b_q^\dagger b_q + b_{-q}^\dagger b_{-q}), \\
H_{e-ph} &= (g/\sqrt{N}) \sum_q \sum_{k,\sigma} [c_{k+q,\sigma}^\dagger c_{k,\sigma} (b_q^\dagger + b_{-q}) + h.c.],
\end{aligned}$$

where H_e is an effective mean-field Hamiltonian with SC and CDW orders. $c_{k,\sigma}^\dagger$ ($c_{k,\sigma}$) is the creation (annihilation) operator for an electron with spin σ and momentum k , ξ_k is the electronic dispersion, Δ_k is the SC order parameter and χ_k is the CDW order parameter with modulation wave-vector Q . H_{ph} is the Hamiltonian for free phonons with phonon creation operator b_q^\dagger for wave-vector q and frequency ω_q . H_{e-ph} is the Hamiltonian describing electron-phonon interaction with strength g and N is the number of lattice sites in the system. The Green's function corresponding to H_e is given by $\hat{G}^{-1}(i\omega_n, k) = (i\omega_n - \hat{H}_e)$ and has a matrix form in the extended Nambu basis $\Psi_k^\dagger = (c_{k,\uparrow}^\dagger, c_{-k,\downarrow}, c_{k+Q,\uparrow}^\dagger, c_{-k-Q,\downarrow})$ which is given by,

$$G^{-1} = \begin{pmatrix} i\omega_n - \xi_k & -\Delta_k & -\chi_k & 0 \\ -\Delta_k^* & i\omega_n + \xi_k & 0 & \chi_k \\ -\chi_k^* & 0 & i\omega_n - \xi_{k+Q} & -\Delta_{k+Q} \\ 0 & \chi_k^* & -\Delta_{k+Q}^* & i\omega_n + \xi_{k+Q} \end{pmatrix}, \quad (2)$$

where ω_n is the Matsubara frequency. We use a band-structure for a prototype cuprate system [55] [see supplementary materials (SM) [56]]. We consider a d-wave symmetric SC gap, given by $\Delta_k = (\Delta_{max}/2)[\cos(k_x) - \cos(k_y)]$, where Δ_{max} denotes the maximum gap. Following several theoretical studies [47, 57, 58] and experimental evidences [20, 59], we consider a CDW order parameter with Q given by the axial wave-vector connecting two neighboring 'hot-spots', the points on Fermi-surface which intersect the magnetic-brillouin zone boundary [41]. Moreover, the CDW gap is taken to have a maximum (χ_{max}) at the hot-spots, falling off exponentially away from the hot-spots [47].

The modified electronic spectrum in the presence of SC and CDW orders will re-normalize the free phonon propagator, $D_0(z, q) = 2\omega_q/(z^2 - \omega_q^2)$. To analyze this, we begin by writing the imaginary time (τ) phonon propagators in matrix form in the ordered phase. The corresponding matrix elements are given by $D_{m,n}(q, \tau) = -\langle \mathcal{T} \phi_{q+mQ}(\tau) \phi_{q+nQ}^\dagger(0) \rangle$, where \mathcal{T} is the time-ordering operator [54], ϕ_q is the phonon field operator given by $b_q^\dagger + b_{-q}$ and $m, n = \pm$. Noting that $D_{++} \equiv D_{--} := D_1(z, q)$ and $D_{+-} \equiv D_{-+} := D_2(z, q)$, within a per-

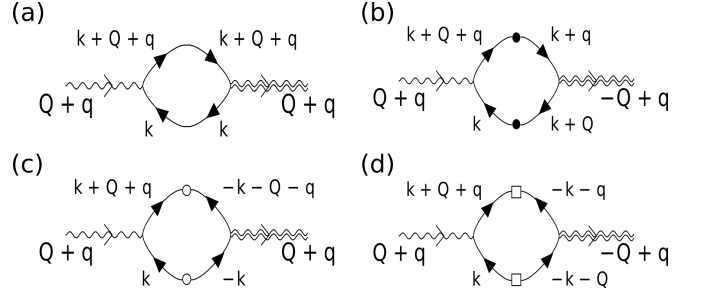


FIG. 2. (a), (b), (c) and (d) represent the Feynman diagrams for the terms in the Dyson equations [Eq. (3)] involving the self-energies Π_1 , Π_2 , Π_3 and Π_4 respectively in the presence of CDW and SC orders.

turbative treatment of electron-phonon interaction, we evaluate the re-normalized phonon propagators D_1 and D_2 by using Dyson equations

$$\begin{aligned}
D_1(z, q) &= D_0(z, q + Q) \left[1 + \Pi_1(z, q) D_1(z, q) + \right. \\
&\quad \left. \Pi_2(z, q) D_1(z, q) + \Pi_3(z, q) D_2(z, q) + \right. \\
&\quad \left. \Pi_4(z, q) D_2(z, q) \right], \quad (3)
\end{aligned}$$

$$\begin{aligned}
D_2(z, q) &= D_0(z, q - Q) \left[\Pi_1(z, q) D_2(z, q) + \Pi_2(z, q) D_2(z, q) \right. \\
&\quad \left. + \Pi_3(z, q) D_1(z, q) + \Pi_4(z, q) D_1(z, q) \right],
\end{aligned}$$

where, $\Pi_{1,2,3,4}(z, q)$ represent the phonon self-energies. The leading contributions to the Dyson equations [Eqs. (3)] are shown in Fig. 2. Explicit expressions for $\Pi_{1,2,3,4}(z, q)$ are presented in the SM [56].

We obtain the new modes for phonon in the ordered phase by decoupling Eq. (3), with the definition $D_\pm(z, q) = D_1(z, q) \pm D_2(z, q)$ and then solving $D_\pm(z, q)$ with the assumption that $\omega_{Q\pm q} \approx \omega_Q$ for small q . Finally, plugging in $D_0(z, q)$, we obtain the solutions as,

$$D_\pm(z, q) = \frac{2\omega_Q}{z^2 - \omega_Q^2 - 2\omega_Q \Pi_\pm(z, q)}, \quad (4)$$

where $\Pi_+ = \Pi_1 + \Pi_2 + \Pi_3 + \Pi_4$ and $\Pi_- = \Pi_1 + \Pi_2 - \Pi_3 - \Pi_4$. The dispersion of the new phonon modes correspond to the values of z , for which denominator of Eq. (4) vanishes. Subsequently, taking only q dependence in Π , the frequency for each mode is given by

$$\Omega_\pm^2(q) = \omega_Q^2 + 2\omega_Q \Pi_\pm(q). \quad (5)$$

These two new phonon modes in Eq. (5) with frequency Ω_\pm signify branching of the free phonon near Q due to presence of CDW and SC orders. We find that the split between Ω_\pm is proportional to the magnitude of the CDW order. Also, we only plot Π_\pm as a function of $\tilde{q} = q - Q$,

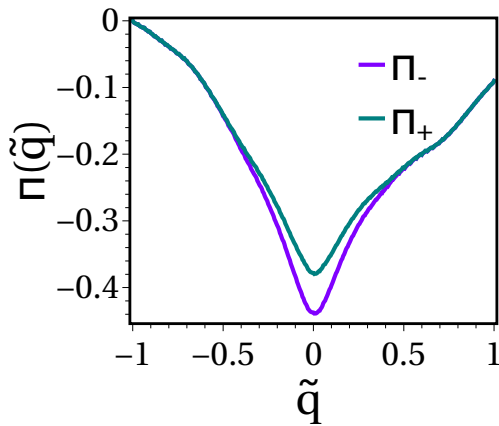


FIG. 3. Plots of the self-energy Π_{\pm} as a function of $\tilde{q} = q - Q$ corresponding to the two re-normalized phonon modes Ω_{\pm} in the presence of $\chi_{max} = 0.05$ and $\Delta_{max} = 0.05$. Both Π_{\pm} exhibit a depletion around $\tilde{q} = 0$, implying a softening in the phonon-dispersion of the two new modes Ω_{\pm} around Q .

as the modes $\Omega_{\pm}(q)$ can be easily identified from the corresponding Π_{\pm} in Eq. (5). For depicting the strength of the phonon-softening, we look at $\Pi_{\pm}(\tilde{q})$ after subtracting $\Pi_{\pm}(\tilde{q} = -1)$. In Fig. 3, we observe that $\Pi_{\pm}(\tilde{q})$ decreases strongly within a finite range around $\tilde{q} = 0$, with a minimum at $\tilde{q} = 0$, readily suggesting a softening of phonon-frequency around Q . We also observe that, away from $\tilde{q} = 0$, $\Pi_{\pm}(\tilde{q})$ goes towards zero, implying a suppression of phonon-softening away from Q . This suggests that the effect of CDW and SC orders on the phonon are maximum at Q , and diminishes away from it. Additionally, we notice that the suppression of Π_{-} is more than the suppression of Π_{+} and the \tilde{q} dependence of Π_{\pm} are extremely similar to each other. Hence, for a simpler presentation, in the rest of the paper, we only plot Π_{-} with \tilde{q} [re-labeled as $\Pi(\tilde{q})$].

So far, we obtain a phonon-softening in the presence of SC and CDW orders. However, to address the anomalous phonon-softening in cuprates, we need to include fluctuation related effects, which are major constituents governing the phase diagram of these systems. For example, such fluctuations can lead to quasi-particle scattering which are known to have vital roles in Fermi-arc related physics of the pseudo-gap phase [60–62]. The strength of the scattering depends on temperature; while it can be large at high temperatures, a sudden reduction occurs below T_c , which can be attributed to a fractionalization of a PDW [47]. To give an idea, the proposal of fractionalization of a PDW order suggests that the fluctuation of a U(1) gauge field gives a constraint connecting SC and CDW. As a result, fractionalization of PDW occurs at an energy scale associated to the pseudo-gap temperature T^* , consequently fluctuations largely increase in the system. However, below T_c , the fluctuations quench, thus yielding a global phase coherence of CDW and SC

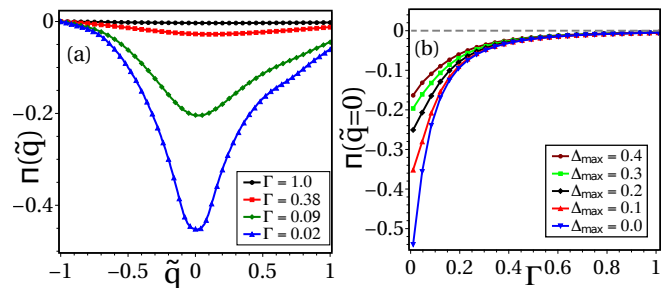


FIG. 4. (a) The variation of $\Pi(\tilde{q})$ with \tilde{q} for four different values of Γ with $\chi_{max} = 0.2$ and $\Delta_{max} = 0$. The plots portray a suppression in phonon-softening with increase in Γ . (b) Plots of $\Pi(\tilde{q} = 0)$ with variation in Γ for five different values of Δ_{max} with $\chi_{max} = 0.2$. The plots manifest a suppression in phonon-softening with an increase in Δ_{max} . The effect of Δ_{max} is strongest for low Γ , and weakest for high Γ .

orders and increasing the life-time of quasi-particles.

In order to study the evolution of the phonon-softening with temperature, we incorporate a finite inverse life-time of quasi-particles, given by Γ , pertinent to the fluctuation related effects in the system. The self-energy in Matsubara frequency due to Γ can be written as $\Sigma = i\Gamma \text{sgn}(\omega_n)$ and the Green's function in Eq. (2) will transform as

$$G_{i,j}^{-1}(i\omega_n, k) \rightarrow G_{i,j}^{-1}(i\omega_n + \Sigma, k). \quad (6)$$

In the presence of Γ , the phonon-dispersion will be modified by the real part of $\Pi(\tilde{q})$, again relabeled as $\Pi(\tilde{q})$. Detailed calculations are presented in the SM [56].

To understand the collective effect of the SC gap and Γ on the phonon-softening, it is important to disentangle the role played by Γ and the SC gap. Therefore, we start by studying the effect of Γ taking $\Delta_{max} = 0$. Fig. 4(a) shows the variation of $\Pi(\tilde{q})$ as a function of \tilde{q} for four different Γ with $\chi_{max} = 0.2$. We notice that for very small value of $\Gamma = 0.02$, there is a significantly strong phonon-softening around $\tilde{q} = 0$. With increasing Γ , the phonon-softening starts to reduce and for a very large $\Gamma = 1.0$, the phonon-softening gets almost fully suppressed. We also observe that the phonon-softening at $\tilde{q} = 0$ is most strongly affected by Γ . Therefore, for rest of the analysis, we will concentrate on Π at $\tilde{q} = 0$ to quantify the phonon-softening.

Now, we inspect the role of the SC order and the interplay between superconductivity and Γ . In Fig. 4(b), we plot the variation of $\Pi(\tilde{q} = 0)$ with Γ , for five different Δ_{max} taking $\chi_{max} = 0.2$. We notice that Δ_{max} has a prominent effect when Γ is very small, as can be seen from the change in $\Pi(\tilde{q} = 0)$ around $\Gamma \sim 0.05$. In this regime, Δ_{max} weakens the softening of phonon. Similar effect on phonons in the SC phase has been indicated in conventional s-wave superconductors [63, 64]. With increasing Γ , for example around $\Gamma \sim 0.3$, the effect of Δ_{max} becomes less significant. Finally, for very large $\Gamma \simeq 1.0$,

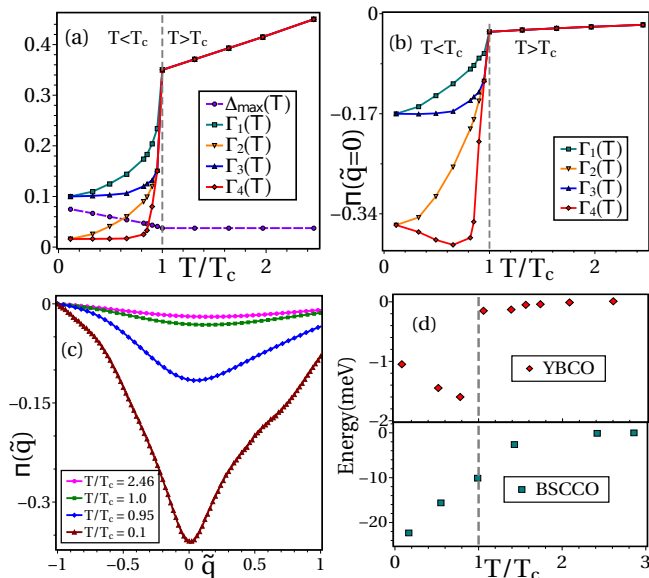


FIG. 5. (a) Different sets of T-dependence for inverse lifetime of quasiparticles denoted by Γ_1 , Γ_2 , Γ_3 and Γ_4 . The T-dependence of the SC gap is denoted by $\Delta_{max}(T)$. In all cases, $\chi_{max} = \Delta_{max}$. (b) The T-dependence of $\Pi(\tilde{q} = 0)$ for different parameter sets in (a). A large negative value of $\Pi(\tilde{q} = 0)$ in the regime $T \lesssim T_c$ implies a strong enhancement of phonon-softening, while $\Pi(\tilde{q} = 0) \rightarrow 0$ implies a strong suppression in phonon-softening in the regime $T > T_c$. (c) The variation of $\Pi(\tilde{q})$ with \tilde{q} at four different temperatures for parameter set Γ_4 and $\Delta_{max}(T)$ shown in (a). (d) Schematic representation of the experimental results of phonon-softening at CDW wave-vector for YBCO and BSCCO, adopted from Refs. [29, 31].

changing Δ_{max} has almost no effect. These results highlight two crucial points. First, both superconductivity and Γ suppress the phonon-softening. Second, the role of Δ_{max} is prominent at low Γ , while negligible for large Γ .

We have seen that the introduction of superconductivity suppresses the phonon-softening, while experiments observe a seemingly opposite characteristic of enhancement of phonon-softening below T_c . At this point, we should also notice that Γ suppresses the phonon-softening, as shown in Fig. 4(a). Moreover, Γ is expected to increase with temperature due to increase in fluctuations, whereas Δ_{max} is expected to decrease with temperature, for example in a simple BCS type scenario. Thus, they behave in opposite manner with temperature.

We consider temperature (T) dependence phenomenologically in Δ_{max} and Γ , similar to the T dependence used in explaining spectral function in ARPES experiments [53]. The T-dependence of Δ_{max} and Γ are shown in Fig. 5(a). Below T_c , Δ_{max} decreases with T, whereas remains approximately constant above T_c . Moreover following indications from Raman spectroscopy [45], χ_{max} is taken to be equal to Δ_{max} . To illustrate how different T-dependence of Γ and Δ_{max} can give different

features in phonon-softening, we use four different types of T-dependence for Γ , denoted by $\Gamma_1, \Gamma_2, \Gamma_3$ and Γ_4 in Fig. 5(a). Note that, they differ in magnitudes compared to Δ_{max} . In all these cases, Γ reduces significantly below T_c , with the strongest fall in Γ_4 and the weakest fall in Γ_1 , but still remains finite even in the limit $T \rightarrow 0$ [65]. Moreover, we considered in all the cases, a linear T-dependence for Γ for $T > T_c$, as suggested in some earlier works [66, 67].

In Fig. 5(b), we plot $\Pi(\tilde{q} = 0)$ for the parameters in Fig. 5(a). We start by closely inspecting the Γ_4 case in Fig. 5(b). We observe that the values of $\Pi(\tilde{q} = 0)$ are close to zero for high temperatures ($T \gg T_c$), implying that the phonon-softening is strongly suppressed. Remarkably, we observe that for temperatures $T \lesssim T_c$, the values of $\Pi(\tilde{q} = 0)$ reduce sharply towards more negative values, which suggest that the phonon-softening enhances strongly. But surprisingly, towards further lower temperatures below T_c , $\Pi(\tilde{q} = 0)$ enhances, which implies a suppression in phonon-softening. However, the phonon-softening below T_c always remains stronger as compared to $T > T_c$. Very similar features have been observed in $\text{YBa}_2\text{Cu}_3\text{O}_{6+y}$ (YBCO) [29], as shown schematically in Fig. 5(d). In Fig. 5(c), we present the full \tilde{q} dependence of Π at four different temperatures for the case Γ_4 . We observe that away from $\tilde{q} = 0$, phonon-softening is less sensitive to the variation of temperature. Similar feature has been found in experiments [29, 31].

Next, we closely investigate the Γ_1 case in Fig. 5(b) for $T \lesssim T_c$. Very interestingly, the features for $T \lesssim T_c$ possess marked differences from Γ_4 case. We notice a smoother enhancement in phonon-softening just below T_c ($T \sim T_c$), while the enhancement is more rapid and sharper for Γ_4 case. In particular, towards lower temperatures ($T \rightarrow 0$), a further enhancement in phonon-softening can be noticed in contrast to the suppression observed for Γ_4 . Analogous features in phonon-softening have been also observed in $\text{Bi}_2\text{Sr}_2\text{CaCu}_2\text{O}_{8+y}$ (BSCCO) [31], schematically presented in Fig. 5(d). To demonstrate the different features in phonon-softening resulting from an intricate interplay between SC gap and Γ below T_c , we plot results for two more cases Γ_2 and Γ_3 , shown in Fig. 5(b). Below T_c , for Γ_2 , phonon-softening sharply enhances than for Γ_3 as $T \rightarrow 0$.

In summary, within a mean-field description of superconductivity and charge-density wave (CDW), describing under-doped cuprates, we obtained a softening of the phonon-dispersion associated to the CDW wave-vector (Q). The crucial finding of our work is that reduced amount of fluctuations in both CDW and superconducting (SC) orders below T_c , can successfully describe the ‘anomalous’ phonon-softening. A reduction in the fluctuations below T_c can be motivated from a recent proposal based on fractionalization of a PDW order [47]. Moreover, we also found that the features of phonon-softening at low temperatures depend on an intricate interplay be-

tween SC order and fluctuations. In this work, we considered the strength of electron-phonon coupling to be momentum (k)-independent. However, the formalism in this work, can easily be extended to include k -dependent electron-phonon coupling. We expect, in such a scenario, the phonon-softening will still occur at Q only below T_c , but the softening will have a different wave-vector dependence around Q . We believe our results can find applications in many two-dimensional materials where an interplay between CDW and SC orders plays an important role and thus opening much broader prospects of our work.

We acknowledge A. Banerjee and Y. Sidis for valuable discussions. This work has received financial support from the ERC, under grant agreement AdG-694651-CHAMPAGNE.

-
- [1] H. Alloul, T. Ohno, and P. Mendels, *Phys. Rev. Lett.* **63**, 1700 (1989).
- [2] W. W. Warren, R. E. Walstedt, G. F. Brennert, R. J. Cava, R. Tycko, R. F. Bell, and G. Dabbagh, *Phys. Rev. Lett.* **62**, 1193 (1989).
- [3] C. Berthier, M. Julien, M. Horvatić, and Y. Berthier, *Journal de Physique I* **6**, 2205 (1996).
- [4] D. S. Marshall, D. S. Dessau, A. G. Loeser, C.-H. Park, A. Y. Matsuura, J. N. Eckstein, I. Bozovic, P. Fournier, A. Kapitulnik, W. E. Spicer, and Z.-X. Shen, *Phys. Rev. Lett.* **76**, 4841 (1996).
- [5] J. M. Harris, P. J. White, Z.-X. Shen, H. Ikeda, R. Yoshizaki, H. Eisaki, S. Uchida, W. D. Si, J. W. Xiong, Z.-X. Zhao, and D. S. Dessau, *Phys. Rev. Lett.* **79**, 143 (1997).
- [6] C. Renner, B. Revaz, J.-Y. Genoud, K. Kadowaki, and O. Fischer, *Phys. Rev. Lett.* **80**, 149 (1998).
- [7] A. Ino, T. Mizokawa, K. Kobayashi, A. Fujimori, T. Sasagawa, T. Kimura, K. Kishio, K. Tamasaku, H. Eisaki, and S. Uchida, *Phys. Rev. Lett.* **81**, 2124 (1998).
- [8] F. Ronning, T. Sasagawa, Y. Kohsaka, K. M. Shen, A. Damascelli, C. Kim, T. Yoshida, N. P. Armitage, D. H. Lu, D. L. Feng, L. L. Miller, H. Takagi, and Z.-X. Shen, *Phys. Rev. B* **67**, 165101 (2003).
- [9] E. Fradkin, S. A. Kivelson, and J. M. Tranquada, *Rev. Mod. Phys.* **87**, 457 (2015).
- [10] C. Pépin, D. Chakraborty, M. Grandadam, and S. Sarkar, *Annual Review of Condensed Matter Physics* **11**, 301 (2020).
- [11] J. E. Hoffman, E. W. Hudson, K. M. Lang, V. Madhavan, H. Eisaki, S. Uchida, and J. C. Davis, *Science* **295**, 466 (2002).
- [12] N. Doiron-Leyraud, C. Proust, D. LeBoeuf, J. Levallois, J.-B. Bonnemaïson, R. Liang, D. A. Bonn, W. N. Hardy, and L. Taillefer, *Nature* **447**, 565 (2007).
- [13] G. Ghiringhelli, M. Le Tacon, M. Minola, S. Blanco-Canosa, C. Mazzoli, N. B. Brookes, G. M. De Luca, A. Frano, D. G. Hawthorn, F. He, T. Loew, M. M. Sala, D. C. Peets, M. Salluzzo, E. Schierle, R. Sutarto, G. A. Sawatzky, E. Weschke, B. Keimer, and L. Braicovich, *Science* **337**, 821 (2012).
- [14] H.-H. Wu, M. Buchholz, C. Trabant, C. Chang, A. Komařek, F. Heigl, M. Zimmermann, M. Cwik, F. Nakamura, M. Braden, *et al.*, *Nature communications* **3**, 1023 (2012).
- [15] A. J. Achkar, R. Sutarto, X. Mao, F. He, A. Frano, S. Blanco-Canosa, M. Le Tacon, G. Ghiringhelli, L. Braicovich, M. Minola, M. Moretti Sala, C. Mazzoli, R. Liang, D. A. Bonn, W. N. Hardy, B. Keimer, G. A. Sawatzky, and D. G. Hawthorn, *Phys. Rev. Lett.* **109**, 167001 (2012).
- [16] E. Blackburn, J. Chang, M. Hücker, A. T. Holmes, N. B. Christensen, R. Liang, D. A. Bonn, W. N. Hardy, U. Rütt, O. Gutowski, M. v. Zimmermann, E. M. Forgan, and S. M. Hayden, *Phys. Rev. Lett.* **110**, 137004 (2013).
- [17] E. Blackburn, J. Chang, A. H. Said, B. M. Leu, R. Liang, D. A. Bonn, W. N. Hardy, E. M. Forgan, and S. M. Hayden, *Phys. Rev. B* **88**, 054506 (2013).
- [18] S. Blanco-Canosa, A. Frano, T. Loew, Y. Lu, J. Porras, G. Ghiringhelli, M. Minola, C. Mazzoli, L. Braicovich, E. Schierle, E. Weschke, M. Le Tacon, and B. Keimer, *Phys. Rev. Lett.* **110**, 187001 (2013).
- [19] T. P. Croft, C. Lester, M. S. Senn, A. Bombardi, and S. M. Hayden, *Phys. Rev. B* **89**, 224513 (2014).
- [20] E. H. da Silva Neto, P. Aynajian, A. Frano, R. Comin, E. Schierle, E. Weschke, A. Gyenis, J. Wen, J. Schneeloch, Z. Xu, S. Ono, G. Gu, M. Le Tacon, and A. Yazdani, *Science* **343**, 393 (2014).
- [21] K. Matsuba, S. Yoshizawa, Y. Mochizuki, T. Mochiku, K. Hirata, and N. Nishida, *Journal of the Physical Society of Japan* **76**, 063704 (2007).
- [22] K. Fujita, C. K. Kim, I. Lee, J. Lee, M. Hamidian, I. A. Firmo, S. Mukhopadhyay, H. Eisaki, S. Uchida, M. J. Lawler, E. A. Kim, and J. C. Davis, *Science* **344**, 612 (2014).
- [23] T. Machida, Y. Kohsaka, K. Matsuoka, K. Iwaya, T. Hanaguri, and T. Tamegai, *Nature communications* **7**, 11747 (2016).
- [24] E. J. Woll and W. Kohn, *Phys. Rev.* **126**, 1693 (1962).
- [25] B. Renker, H. Rietschel, L. Pintschovius, W. Gläser, P. Brüesch, D. Kuse, and M. J. Rice, *Phys. Rev. Lett.* **30**, 1144 (1973).
- [26] K. Carneiro, G. Shirane, S. A. Werner, and S. Kaiser, *Phys. Rev. B* **13**, 4258 (1976).
- [27] J. P. Pouget, B. Hennion, C. Escribe-Filippini, and M. Sato, *Phys. Rev. B* **43**, 8421 (1991).
- [28] J. Wilson, F. Di Salvo, and S. Mahajan, *Advances in Physics* **50**, 1171 (2001).
- [29] M. Le Tacon, A. Bosak, S. M. Souliou, G. Dellea, T. Loew, R. Heid, K.-P. Bohnen, G. Ghiringhelli, M. Krisch, and B. Keimer, *Nat. Phys.* **10**, 52 (2014).
- [30] H. Miao, D. Ishikawa, R. Heid, M. Le Tacon, G. Fabbris, D. Meyers, G. D. Gu, A. Q. R. Baron, and M. P. M. Dean, *Phys. Rev. X* **8**, 011008 (2018).
- [31] W. Lee, K. Zhou, M. Hepting, J. Li, A. Nag, A. Walters, M. Garcia-Fernandez, H. Robarts, M. Hashimoto, H. Lu, *et al.*, arXiv preprint arXiv:2007.02464 (2020).
- [32] R. J. McQueeney, Y. Petrov, T. Egami, M. Yethiraj, G. Shirane, and Y. Endoh, *Phys. Rev. Lett.* **82**, 628 (1999).
- [33] H. Uchiyama, A. Q. R. Baron, S. Tsutsui, Y. Tanaka, W.-Z. Hu, A. Yamamoto, S. Tajima, and Y. Endoh, *Phys. Rev. Lett.* **92**, 197005 (2004).

- [34] D. Reznik, T. Fukuda, D. Lamago, A. Baron, S. Tsutsui, M. Fujita, and K. Yamada, *Journal of Physics and Chemistry of Solids* **69**, 3103 (2008).
- [35] J. Graf, M. d'Astuto, C. Jozwiak, D. R. Garcia, N. L. Saini, M. Krisch, K. Ikeuchi, A. Q. R. Baron, H. Eisaki, and A. Lanzara, *Phys. Rev. Lett.* **100**, 227002 (2008).
- [36] M. d'Astuto, G. Dhahlenne, J. Graf, M. Hoesch, P. Giura, M. Krisch, P. Berthet, A. Lanzara, and A. Shukla, *Phys. Rev. B* **78**, 140511 (2008).
- [37] A. Q. Baron, J. P. Sutter, S. Tsutsui, H. Uchiyama, T. Masui, S. Tajima, R. Heid, and K.-P. Bohnen, *Journal of Physics and Chemistry of Solids* **69**, 3100 (2008).
- [38] M. Raichle, D. Reznik, D. Lamago, R. Heid, Y. Li, M. Bakr, C. Ulrich, V. Hinkov, K. Hradil, C. T. Lin, and B. Keimer, *Phys. Rev. Lett.* **107**, 177004 (2011).
- [39] J. Lorenzo, R. Currat, P. Monceau, B. Hennion, H. Berger, and F. Levy, *Journal of Physics: Condensed Matter* **10**, 5039 (1998).
- [40] H. Requardt, J. E. Lorenzo, P. Monceau, R. Currat, and M. Krisch, *Phys. Rev. B* **66**, 214303 (2002).
- [41] K. B. Efetov, H. Meier, and C. Pépin, *Nat. Phys.* **9**, 442 (2013).
- [42] L. E. Hayward, D. G. Hawthorn, R. G. Melko, and S. Sachdev, *Science* **343**, 1336 (2014).
- [43] Y. Wang, D. F. Agterberg, and A. Chubukov, *Phys. Rev. Lett.* **114**, 197001 (2015).
- [44] D. Chakraborty, C. Morice, and C. Pépin, *Physical Review B* **97**, 214501 (2018).
- [45] B. Loret, N. Auvray, Y. Gallais, M. Cazayous, A. Forget, D. Colson, M.-H. Julien, I. Paul, M. Civelli, and A. Sacuto, *Nature Physics* , 1 (2019).
- [46] J. Chang, E. Blackburn, A. T. Holmes, N. B. Christensen, J. Larsen, J. Mesot, R. Liang, D. A. Bonn, W. N. Hardy, A. Watenphul, M. v. Zimmermann, E. M. Forgan, and S. M. Hayden, *Nat. Phys.* **8**, 871 (2012).
- [47] D. Chakraborty, M. Grandadam, M. H. Hamidian, J. C. S. Davis, Y. Sidis, and C. Pépin, *Phys. Rev. B* **100**, 224511 (2019).
- [48] S. D. Edkins, A. Kostin, K. Fujita, A. P. Mackenzie, H. Eisaki, S. Uchida, S. Sachdev, M. J. Lawler, E.-A. Kim, J. S. Davis, *et al.*, *Science* **364**, 976 (2019).
- [49] M. Hamidian, S. Edkins, S. H. Joo, A. Kostin, H. Eisaki, S. Uchida, M. Lawler, E.-A. Kim, A. Mackenzie, K. Fujita, *et al.*, *Nature* **532**, 343 (2016).
- [50] M. Norman, H. Ding, M. Randeria, J. Campuzano, T. Yokoya, T. Takeuchi, T. Takahashi, T. Mochiku, K. Kadowaki, P. Guptasarma, *et al.*, *Nature* **392**, 157 (1998).
- [51] M. R. Norman and C. Pépin, *Rep. Prog. Phys.* **66**, 1547 (2003).
- [52] M. Grandadam, D. Chakraborty, X. Montiel, and C. Pépin, arXiv preprint arXiv:2002.12622 (2020).
- [53] M. R. Norman, M. Randeria, H. Ding, and J. C. Campuzano, *Phys. Rev. B* **57**, R11093 (1998).
- [54] P. Lee, T. Rice, and P. Anderson, *Solid State Communications* **88**, 1001 (1993).
- [55] C. Berthod, I. Maggio-Aprile, J. Bruér, A. Erb, and C. Renner, *Phys. Rev. Lett.* **119**, 237001 (2017).
- [56] S. Sarkar, M. Grandadam, and C. Pépin, *Supplementary materials*.
- [57] Y. Wang and A. Chubukov, *Physical Review B* **90**, 2113 (2014).
- [58] D. Chowdhury and S. Sachdev, *Phys. Rev. B* **90**, 134516 (2014).
- [59] R. Comin, A. Frano, M. M. Yee, Y. Yoshida, H. Eisaki, E. Schierle, E. Weschke, R. Sutarto, F. He, A. Soumyanarayanan, Y. He, M. Le Tacon, I. S. Elfimov, J. E. Hoffman, G. A. Sawatzky, B. Keimer, and A. Damascelli, *Science* **343**, 390 (2014).
- [60] M. R. Norman, M. Randeria, H. Ding, and J. C. Campuzano, *Phys. Rev. B* **52**, 615 (1995).
- [61] M. R. Norman, A. Kanigel, M. Randeria, U. Chatterjee, and J. C. Campuzano, *Phys. Rev. B* **76**, 174501 (2007).
- [62] E. G. Dalla Torre, Y. He, D. Benjamin, and E. Demler, *New Journal of Physics* **17**, 022001 (2015).
- [63] J. D. Axe and G. Shirane, *Phys. Rev. B* **8**, 1965 (1973).
- [64] D. Reznik, *Physica C: Superconductivity* **481**, 75 (2012).
- [65] A. Chubukov, M. Norman, A. Millis, and E. Abrahams, *Physical Review B* **76**, 180501 (2007).
- [66] A. Kanigel, M. Norman, M. Randeria, U. Chatterjee, S. Souma, A. Kaminski, H. Fretwell, S. Rosenkranz, M. Shi, T. Sato, *et al.*, *Nature Physics* **2**, 447 (2006).
- [67] C. M. Varma, P. B. Littlewood, S. Schmitt-Rink, E. Abrahams, and A. E. Ruckenstein, *Phys. Rev. Lett.* **63**, 1996 (1989).

Supplementary materials for

Anomalous softening of phonon-dispersion in cuprate superconductors

Saheli Sarkar,¹ Maxence Grandadam,¹ and Catherine Pépin¹

¹*Institut de Physique Théorique, Université Paris-Saclay, CEA, CNRS, F-91191 Gif-sur-Yvette, France.*

THE MODEL AND PARAMETERS

In this section, we discuss the model describing the cuprate in the presence of charge-density wave (CDW) and superconducting (SC) orders. To analyze the phonon-dispersion in the presence of CDW and SC orders, we start with a total Hamiltonian H_{tot} , which incorporates an effective mean-field electronic Hamiltonian (H_e) describing CDW and SC orders, Hamiltonian for free phonons (H_{ph}) and electron-phonon interaction Hamiltonian (H_{e-ph}) as given in Eq. (1) of the main text. The inverse Green's function matrix $\hat{G}^{-1}(i\omega_n, k) = (i\omega_n - \hat{H}_e)$ corresponding to the Hamiltonian H_e in extended Nambu basis $\Psi_k^\dagger = (c_{k,\uparrow}^\dagger, c_{-k,\downarrow}, c_{k+Q,\uparrow}^\dagger, c_{-k-Q,\downarrow})$ is given by,

$$G^{-1}(i\omega_n, k) = \begin{pmatrix} i\omega_n - \xi_k & -\Delta_k & -\chi_k & 0 \\ -\Delta_k^* & i\omega_n + \xi_k & 0 & \chi_k \\ -\chi_k^* & 0 & i\omega_n - \xi_{k+Q} & -\Delta_{k+Q} \\ 0 & \chi_k^* & -\Delta_{k+Q}^* & i\omega_n + \xi_{k+Q} \end{pmatrix}, \quad (S1)$$

where, ξ_k is the electronic dispersion dispersion, given by, $\xi_k = 2t_1[\cos k_x + \cos k_y] + 4t_2 \cos(k_x) \cos(k_y) + 2t_3(\cos(2k_x) + \cos(2k_y)) - \mu$, with $t_1 = -70.25$ meV, $t_2 = 34.75$ meV, $t_3 = -11$ meV and $\mu = -89$ meV. In this paper, all energy scales are expressed in units of t_1 . Δ_k is the SC order parameter and χ_k is the CDW order parameter with finite wave-vector Q . ω_n is the Matsubara frequency. Ψ is the Nambu spinor, $c_{k,\uparrow}^\dagger$ is the creation operator for an electronic state with wave-vector k and up spin and $c_{-k,\downarrow}$ is the annihilation operator for an electronic state with wave-vector $-k$ and down spin. The Fermi-surface for the electronic dispersion ξ_k , 'hot-spots' and the CDW wave vectors (Q) parallel to the crystallographic axes are shown in Fig. S1.

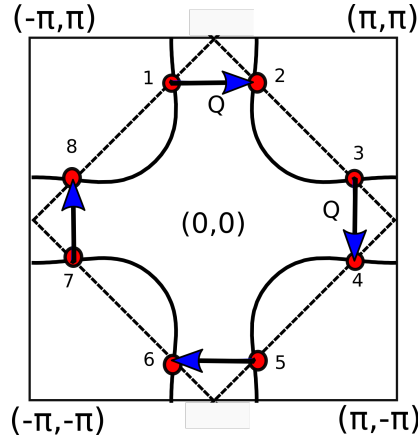


FIG. S1: Fermi surface for a prototype cuprate band structure. The solid black curves represent the Fermi-surface associated to the dispersion ξ_k . The dashed black lines represent the magnetic Brillouin zone boundary of the system. The intersection of the magnetic Brillouin zone boundary and the Fermi-surface are marked by red dots, representing the 'hot-spots' on the Fermi-surface. The CDW modulation wave vector Q , indicated by the arrows are considered to be parallel to the crystallographic axes are shown in the figure.

DYSON EQUATIONS AND CALCULATION OF THE SELF-ENERGY II

In this section, we present the derivation of the phonon propagators, re-normalized due to CDW and SC orders. The free phonon is given by the propagator $D_0(z, q) = 2\omega_q/(z^2 - \omega_q^2)$, where ω_q is the frequency of the phonon mode

for wave-vector q and z is a complex frequency ($\text{Im } z > 0$). The CDW and SC orders will couple to the free-phonon, modifying the propagator, which will consequently give rise to phonon modes with re-normalized dispersion. To evaluate the re-normalized dispersions, we start with Matsubara phonon propagator in matrix form whose elements are given by $D_{m,n}(q, \tau) = -\langle \mathcal{T} \phi_{q+mQ}(\tau) \phi_{q+nQ}^\dagger(0) \rangle$, where \mathcal{T} is the time-ordering operator, and $m, n = \pm$. By noting that $D_{++} \equiv D_{--} := D_1(z, q)$ and $D_{+-} \equiv D_{-+} := D_2(z, q)$, within a perturbative approach for the electron-phonon interaction in Hamiltonian of Eq. (1) in the main text, the Dyson's equations involving self-energies in the presence of SC and CDW orders will give the modified phonon propagators D_1, D_2 and can be written as,

$$\begin{aligned} D_1(z, q) &= D_0(z, q + Q) \left[1 + \Pi_1(z, q)D_1(z, q) + \Pi_1(z, q)D_1(z, q) + \Pi_3(z, q)D_2(z, q) + \Pi_4(z, q)D_2(z, q) \right], \\ D_2(z, q) &= D_0(z, q - Q) \left[\Pi_5(z, q)D_2(z, q) + \Pi_6(z, q)D_2(z, q) + \Pi_7(z, q)D_1(z, q) + \Pi_8(z, q)D_1(z, q) \right]. \end{aligned} \quad (\text{S2})$$

The self-energies $\Pi_1, \Pi_2, \Pi_3, \Pi_4, \Pi_5, \Pi_6, \Pi_7$ and Π_8 in Eq. S2, are given by,

$$\begin{aligned} \Pi_1(\omega, q) &= \frac{g^2}{N} \sum_{k, i\omega_n} [G_{11}(k, i\omega_n)G_{33}(k + q, i\omega_n + i\epsilon_n) + (k \rightarrow k - q)] \\ \Pi_2(\omega, q) &= \frac{g^2}{N} \sum_{k, i\omega_n} [G_{12}(k, i\omega_n)G_{34}(k + q, i\omega_n + i\epsilon_n) + (k \rightarrow k - q)] \\ \Pi_3(\omega, q) &= \frac{g^2}{N} \sum_{k, i\omega_n} [G_{13}(k, i\omega_n)G_{31}(k + q, i\omega_n + i\epsilon_n) + (k \rightarrow k - q)] \\ \Pi_4(\omega, q) &= \frac{g^2}{N} \sum_{k, i\omega_n} [G_{14}(k, i\omega_n)G_{32}(k + q, i\omega_n + i\epsilon_n) + (k \rightarrow k - q)] \\ \Pi_5(\omega, q) &= \frac{g^2}{N} \sum_{k, i\omega_n} [G_{33}(k, i\omega_n)G_{11}(k + q, i\omega_n + i\epsilon_n) + (k \rightarrow k - q)] \\ \Pi_6(\omega, q) &= \frac{g^2}{N} \sum_{k, i\omega_n} [G_{34}(k, i\omega_n)G_{12}(k + q, i\omega_n + i\epsilon_n) + (k \rightarrow k - q)] \\ \Pi_7(\omega, q) &= \frac{g^2}{N} \sum_{k, i\omega_n} [G_{31}(k, i\omega_n)G_{13}(k + q, i\omega_n + i\epsilon_n) + (k \rightarrow k - q)] \\ \Pi_8(\omega, q) &= \frac{g^2}{N} \sum_{k, i\omega_n} [G_{32}(k, i\omega_n)G_{14}(k + q, i\omega_n + i\epsilon_n) + (k \rightarrow k - q)]. \end{aligned} \quad (\text{S3})$$

With a further assumption of small q , we note that $\Pi_1 \approx \Pi_5, \Pi_2 \approx \Pi_6, \Pi_3 \approx \Pi_7$ and $\Pi_4 \approx \Pi_8$, which gives the final form of the Dyson's equations as

$$\begin{aligned} D_1(z, q) &= D_0(z, q + Q) \left[1 + \Pi_1(z, q)D_1(z, q) + \Pi_2(z, q)D_1(z, q) + \Pi_3(z, q)D_2(z, q) + \Pi_4(z, q)D_2(z, q) \right], \\ D_2(z, q) &= D_0(z, q - Q) \left[\Pi_1(z, q)D_2(z, q) + \Pi_2(z, q)D_2(z, q) + \Pi_3(z, q)D_1(z, q) + \Pi_4(z, q)D_1(z, q) \right]. \end{aligned} \quad (\text{S4})$$

The corresponding Feynman-diagrams for the above self-energies in Eq. (S4) are shown in Fig. (2) of the main text. In Eq. (S4), we consider the strength of electron-phonon interaction, g to be k -independent and the number of lattice sites in the system to be N . The Dyson's equations from D_1 and D_2 can be decoupled to obtain the new re-normalized phonon modes, by introducing $D_\pm(z, q) = D_1(z, q) \pm D_2(z, q)$ and then solve for D_\pm . The solution for the frequencies of the new phonon modes are,

$$\Omega_\pm^2(q) = \omega_Q^2 + 2\omega_Q\Pi_\pm(q), \quad (\text{S5})$$

where, $\Omega_\pm(q)$ represent the re-normalized frequencies [also given in Eq. (5) of the main text], and $\Pi_+ = \Pi_1 + \Pi_2 + \Pi_3 + \Pi_4$ and $\Pi_- = \Pi_1 + \Pi_2 - \Pi_3 - \Pi_4$. The Green's function matrix elements $[G(i, j)]$ that are appearing in the

self-energy expressions in Eq. (S4), are given by,

$$\begin{aligned}
G_{11}(k, i\omega_n) &= \frac{A_1}{(i\omega_n + E_k^-)} + \frac{A_2}{(E_k^- - i\omega_n)} + \frac{A_3}{(E_k^+ + i\omega_n)} + \frac{A_4}{(E_k^+ - i\omega_n)}, \\
G_{33}(k, i\omega_n) &= \frac{A_5}{(i\omega_n + E_k^-)} + \frac{A_6}{(E_k^- - i\omega_n)} + \frac{A_7}{(E_k^+ + i\omega_n)} + \frac{A_8}{(E_k^+ - i\omega_n)}, \\
G_{12}(k, i\omega_n) &= \frac{A_9}{(i\omega_n + E_k^-)} + \frac{A_{10}}{(E_k^- - i\omega_n)} + \frac{A_{11}}{(E_k^+ + i\omega_n)} + \frac{A_{12}}{(E_k^+ - i\omega_n)}, \\
G_{34}(k, i\omega_n) &= \frac{A_{13}}{(i\omega_n + E_k^-)} + \frac{A_{14}}{(E_k^- - i\omega_n)} + \frac{A_{15}}{(E_k^+ + i\omega_n)} + \frac{A_{16}}{(E_k^+ - i\omega_n)}, \\
G_{13}(k, i\omega_n) &= \frac{A_{17}}{(i\omega_n + E_k^-)} + \frac{A_{18}}{(E_k^- - i\omega_n)} + \frac{A_{19}}{(E_k^+ + i\omega_n)} + \frac{A_{20}}{(E_k^+ - i\omega_n)}, \\
G_{31}(k, i\omega_n) &= \frac{A_{21}}{(i\omega_n + E_k^-)} + \frac{A_{22}}{(E_k^- - i\omega_n)} + \frac{A_{23}}{(E_k^+ + i\omega_n)} + \frac{A_{24}}{(E_k^+ - i\omega_n)}, \\
G_{14}(k, i\omega_n) &= \frac{A_{25}}{(i\omega_n + E_k^-)} + \frac{A_{26}}{(E_k^- - i\omega_n)} + \frac{A_{27}}{(E_k^+ + i\omega_n)} + \frac{A_{28}}{(E_k^+ - i\omega_n)}, \\
G_{32}(k, i\omega_n) &= \frac{A_{29}}{(i\omega_n + E_k^-)} + \frac{A_{30}}{(E_k^- - i\omega_n)} + \frac{A_{31}}{(E_k^+ + i\omega_n)} + \frac{A_{32}}{(E_k^+ - i\omega_n)},
\end{aligned} \tag{S6}$$

where, E_k^\pm is the re-normalized electronic dispersion and is given by,

$$E_k^\pm = \pm \frac{1}{\sqrt{2}} \sqrt{\beta_k^2 - \eta_k} \tag{S7}$$

with,

$$\begin{aligned}
\beta_k^2 &= E_{1k}^2 + E_{2k}^2 + \Delta_{1k}^2 + \Delta_{2k}^2 + 2\chi_k^2, \\
\eta_k^2 &= [(E_{1k} + E_{2k})(E_{1k} - E_{2k}) + (\Delta_{1k} + \Delta_{2k})(\Delta_{1k} - \Delta_{2k})]^2 \\
&\quad + 4\chi_k^2 [(E_{1k} + E_{2k})^2 + (\Delta_{1k} - \Delta_{2k})^2],
\end{aligned}$$

where we use the following simplified notations, $\xi_k = E_{1k}$, $\xi_{k+Q} = E_{2k}$, $\Delta_k = \Delta_{1k}$ and $\Delta_{k+Q} = \Delta_{2k}$. In the right hand side of the Eq. (S6), the numerators are given by,

$$\begin{aligned}
A_1 &= \frac{(E_{1k} - E_k^-)(E_{2k}^2 - (E_k^-)^2 + \Delta_{2k}^2) - (E_{2k} + E_k^-)\chi_k^2}{2E_k^-(E_k^- - E_k^+)(E_k^- + E_k^+)}, \\
A_2 &= \frac{(E_{1k} + E_k^-)(E_{2k}^2 - (E_k^-)^2 + \Delta_{2k}^2) + (-E_{2k} + E_k^-)\chi_k^2}{2E_k^-(E_k^- - E_k^+)(E_k^- + E_k^+)}, \\
A_3 &= \frac{-(E_{1k} - E_k^+)(E_{2k}^2 - (E_k^+)^2 + \Delta_{2k}^2) + (E_{2k} + E_k^+)\chi_k^2}{2E_k^+(E_k^- - E_k^+)(E_k^- + E_k^+)}, \\
A_4 &= \frac{-(E_{1k} + E_k^+)(E_{2k}^2 - (E_k^+)^2 + \Delta_{2k}^2) + (E_{2k} - E_k^+)\chi_k^2}{2E_k^+(E_k^- - E_k^+)(E_k^- + E_k^+)}, \\
A_5 &= \frac{(E_{2k} - E_k^-)(E_{1k}^2 - (E_k^-)^2 + \Delta_{1k}^2) - (E_{1k} + E_k^-)\chi_k^2}{2E_k^-(E_k^- - E_k^+)(E_k^- + E_k^+)}, \\
A_6 &= \frac{(E_{2k} + E_k^-)(E_{1k}^2 - (E_k^-)^2 + \Delta_{1k}^2) + (-E_{1k} + E_k^-)\chi_k^2}{2E_k^-(E_k^- - E_k^+)(E_k^- + E_k^+)}, \\
A_7 &= \frac{-(E_{2k} - E_k^+)(E_{1k}^2 - (E_k^+)^2 + \Delta_{1k}^2) + (E_{1k} + E_k^+)\chi_k^2}{2E_k^+(E_k^- - E_k^+)(E_k^- + E_k^+)}, \\
A_8 &= \frac{-(E_{2k} + E_k^+)(E_{1k}^2 - (E_k^+)^2 + \Delta_{1k}^2) + (E_{1k} - E_k^+)\chi_k^2}{2E_k^+(E_k^- - E_k^+)(E_k^- + E_k^+)},
\end{aligned}$$

$$\begin{aligned}
A_9 &= \frac{\Delta_{1k}(E_{2k}^2 - (E_k^-)^2 + \Delta_{2k}^2) + \Delta_{2k}\chi_k^2}{2E_k^-(E_k^- - E_k^+)(E_k^- + E_k^+)}, \\
A_{10} &= \frac{\Delta_{1k}(E_{2k}^2 - (E_k^-)^2 + \Delta_{2k}^2) + \Delta_{2k}\chi_k^2}{2E_k^-(E_k^- - E_k^+)(E_k^- + E_k^+)}, \\
A_{11} &= (-1) \frac{\Delta_{1k}(E_{2k}^2 - (E_k^+)^2 + \Delta_{2k}^2) + (\Delta_{2k})\chi_k^2}{2E_k^+(E_k^- - E_k^+)(E_k^- + E_k^+)}, \\
A_{12} &= (-1) \frac{\Delta_{1k}(E_{2k}^2 - (E_k^+)^2 + \Delta_{2k}^2) + (\Delta_{2k})\chi_k^2}{2E_k^+(E_k^- - E_k^+)(E_k^- + E_k^+)},
\end{aligned}$$

$$\begin{aligned}
A_{13} &= \frac{\Delta_{2k}(E_{1k}^2 - (E_k^-)^2 + \Delta_{1k}^2) + \Delta_{1k}\chi_k^2}{2E_k^-(E_k^- - E_k^+)(E_k^- + E_k^+)}, \\
A_{14} &= \frac{\Delta_{2k}(E_{1k}^2 - (E_k^-)^2 + \Delta_{1k}^2) + \Delta_{1k}\chi_k^2}{2E_k^-(E_k^- - E_k^+)(E_k^- + E_k^+)}, \\
A_{15} &= (-1) \frac{\Delta_{2k}(E_{1k}^2 - (E_k^+)^2 + \Delta_{1k}^2) + (\Delta_{1k})\chi_k^2}{2E_k^+(E_k^- - E_k^+)(E_k^- + E_k^+)}, \\
A_{16} &= (-1) \frac{\Delta_{2k}(E_{1k}^2 - (E_k^+)^2 + \Delta_{1k}^2) + (\Delta_{1k})\chi_k^2}{2E_k^+(E_k^- - E_k^+)(E_k^- + E_k^+)},
\end{aligned}$$

$$\begin{aligned}
A_{17} &= \frac{\chi_k[(E_{1k} - E_k^-)(-E_{2k} + E_k^-) + \Delta_{1k}\Delta_{2k} + \chi_k^2]}{2E_k^-(E_k^- - E_k^+)(E_k^- + E_k^+)}, \\
A_{18} &= \frac{\chi_k[-(E_{1k} + E_k^-)(E_{2k} + E_k^-) + \Delta_{1k}\Delta_{2k} + \chi_k^2]}{2E_k^-(E_k^- - E_k^+)(E_k^- + E_k^+)}, \\
A_{19} &= (-1) \frac{\chi_k[(E_{1k} - E_k^+)(-E_{2k} + E_k^+) + \Delta_{1k}\Delta_{2k} + \chi_k^2]}{2E_k^+(E_k^- - E_k^+)(E_k^- + E_k^+)}, \\
A_{20} &= \frac{\chi_k[(E_{1k} + E_k^+)(E_{2k} + E_k^+) - \Delta_{1k}\Delta_{2k} - \chi_k^2]}{2E_k^+(E_k^- - E_k^+)(E_k^- + E_k^+)},
\end{aligned}$$

$$A_{21} = A_{17},$$

$$A_{22} = A_{18},$$

$$A_{23} = A_{19},$$

$$A_{24} = A_{20},$$

$$A_{25} = (-1) \frac{\chi_k[(E_{2k} + E_k^-)(\Delta_{1k}) + E_{1k}\Delta_{2k} - E_k^- \Delta_{2k}]}{2E_k^-(E_k^- - E_k^+)(E_k^- + E_k^+)},$$

$$A_{26} = (-1) \frac{\chi_k[(E_{2k} - E_k^-)(\Delta_{1k}) + E_{1k}\Delta_{2k} + E_k^- \Delta_{2k}]}{2E_k^-(E_k^- - E_k^+)(E_k^- + E_k^+)},$$

$$A_{27} = \frac{\chi_k[(E_{2k} + E_k^+)(\Delta_{1k}) + E_{1k}\Delta_{2k} - E_k^+ \Delta_{2k}]}{2E_k^+(E_k^- - E_k^+)(E_k^- + E_k^+)},$$

$$A_{28} = \frac{\chi_k[(E_{2k} - E_k^+)(\Delta_{1k}) + E_{1k}\Delta_{2k} + E_k^+ \Delta_{2k}]}{2E_k^+(E_k^- - E_k^+)(E_k^- + E_k^+)},$$

$$\begin{aligned}
A_{29} &= (-1) \frac{\chi_k [(E_{2k} + E_k^-)(\Delta_{1k}) + E_{1k}\Delta_{2k} - E_k^- \Delta_{2k}]}{2E_k^- (E_k^- - E_k^+) (E_k^- + E_k^+)}, \\
A_{30} &= (-1) \frac{\chi_k [(E_{2k} - E_k^-)(\Delta_{1k}) + E_{1k}\Delta_{2k} + E_k^- \Delta_{2k}]}{2E_k^- (E_k^- - E_k^+) (E_k^- + E_k^+)}, \\
A_{31} &= \frac{\chi_k [(E_{2k} + E_k^+)(\Delta_{1k}) + E_{1k}\Delta_{2k} - E_k^+ \Delta_{2k}]}{2E_k^+ (E_k^- - E_k^+) (E_k^- + E_k^+)}, \\
A_{32} &= \frac{\chi_k [(E_{2k} - E_k^+)(\Delta_{1k}) + E_{1k}\Delta_{2k} + E_k^+ \Delta_{2k}]}{2E_k^+ (E_k^- - E_k^+) (E_k^- + E_k^+)}.
\end{aligned}$$

To evaluate the self-energies (Π) in Eq. (S3), we first perform the summation over the Matsubara frequency using analytic tool of contour integration. Next, we do the summation over k using numerical tools taking $\Delta_k = \Delta_{k+Q}$, $g = 1$ and $N = 40000$. The plot of the self-energy in this case is presented in Fig. (3) in the main text.

CALCULATION OF SELF-ENERGY Π IN THE PRESENCE OF INVERSE LIFE-TIME Γ

In this section, we present the self-energy calculation in the presence of finite inverse life-time (Γ) of the quasi-particles, associated to thermal fluctuations. Here, Green's function elements become,

$$G_{i,j}(i\omega_n, k) \rightarrow G_{i,j}(i\omega_n + i\Gamma \text{sgn}(\omega_n), k).$$

The self-energies Π in Eq. (S3) now have the following general structure:

$$\sum_{k, i\omega_n} G_k^a(i\omega_n + i\Gamma \text{sgn}(\omega_n)) G_{k+q}^b(i\omega_n + i\Gamma \text{sgn}(\omega_n) + i\epsilon_n), \quad (\text{S8})$$

where, either of 'a' and 'b' symbolically represents the $(i, j)^{th}$ element of the Green's function matrix. To evaluate the Matsubara summation in this case, we need to use a contour avoiding the branch cuts defined by $Im(z) = 0$ and $Im(z + i\epsilon_n) = 0$ as shown in the Fig. S2. Using this contour, we arrive at the following integrations,

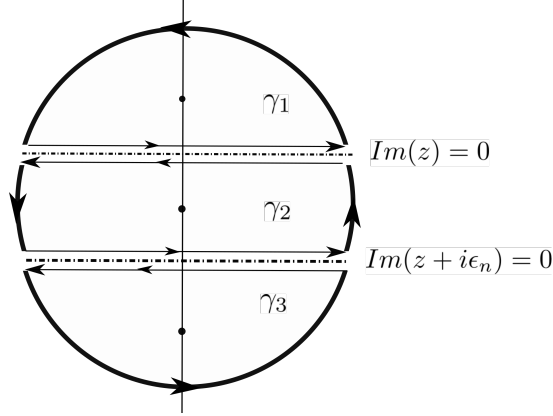


FIG. S2: Contour for complex Matsubara frequency summation: $Im(z) = 0$ and $Im(z + i\epsilon_n) = 0$ denote the two branch-cuts in the complex plane. γ_1 , γ_2 and γ_3 are the three contours of integration.

$$\begin{aligned}
I_{\gamma_1} &= \sum_k \left[\int_{-\infty}^{\infty} \frac{d\omega}{2\pi i} n_F(\omega) G_k^a(\omega + i\Gamma) G_{k+q}^b(\omega + \epsilon + i\Gamma) \right], \\
I_{\gamma_3} &= - \sum_k \left[\int_{-\infty}^{\infty} \frac{d\omega}{2\pi i} n_F(\omega) G_k^a(\omega - \epsilon - i\Gamma) G_{k+q}^b(\omega - i\Gamma) \right], \\
I_{\gamma_2} &= \sum_k \left[\int_{-\infty}^{\infty} \frac{d\omega}{2\pi i} n_F(\omega) \{ G_k^a(\omega - \epsilon - i\Gamma) G_{k+q}^b(\omega + i\Gamma) - G_k^a(\omega - i\Gamma) G_{k+q}^b(\omega + \epsilon + i\Gamma) \} \right],
\end{aligned} \quad (\text{S9})$$

where, $n_F(\omega) = 1/(\exp \beta\omega + 1)$ is the Fermi-distribution function. Moreover $\beta = 1/k_B T$, where k_B is the Boltzmann constant.

Next, in the limit $T \rightarrow 0$, the integrals I_{γ_1} and I_{γ_3} in Eq. (S9) become,

$$\begin{aligned} I_{\gamma_1} &= \sum_k \left[\int_{-\infty}^0 \frac{d\omega}{2\pi i} G_k^a(\omega + i\Gamma) G_{k+q}^b(\omega + \epsilon + i\Gamma) \right] \\ I_{\gamma_3} &= - \sum_k \left[\int_{-\infty}^0 \frac{d\omega}{2\pi i} G_k^a(\omega - \epsilon - i\Gamma) G_{k+q}^b(\omega - i\Gamma) \right]. \end{aligned} \quad (\text{S10})$$

We replace $\omega \rightarrow \omega + \epsilon$ in the first term of I_{γ_2} and successively use

$$\lim_{\epsilon \rightarrow 0} \frac{n_F(\omega + \epsilon) - n_F(\omega)}{\epsilon} = -\delta(\omega),$$

where $\delta(\omega)$ is a Dirac delta function with the property, $\int_{-\infty}^{\infty} d\omega f(\omega) \delta(\omega) = f(0)$. Thus, I_{γ_2} in Eq. (S9) becomes,

$$I_{\gamma_2} = \sum_k \frac{-\epsilon}{2\pi i} [G_k^a(i\Gamma) G_{k+q}^b(\epsilon + i\Gamma)]. \quad (\text{S11})$$

Finally, we evaluate the real frequency (ω) integration in Eq. (S10) for each of the four self-energies Π_1 , Π_2 , Π_3 and Π_4 in Eq. (S3) by using,

$$\int_{-\infty}^0 d\omega \left[\frac{1}{(\omega - x) * (\omega - y)} \right] = \frac{\log[x] - \log[y]}{x - y}, \quad (\text{S12})$$

where, $x, y \in \mathbb{C}$. The summation over k is again evaluated using numerical tools. The re-normalization of phonon-spectrum in this case is given by the real part of the self-energy. The real part of the self-energy are plotted for different set of SC order, Γ and CDW order in Fig. (4) and Fig. (5) of the main text.